Chalcogenide Letters Vol. 13, No. 8, August 2016, p. 389 - 396

PHYSICAL PROPERTIES OF In_2S_3 THIN FILMS GROWN BY CHEMICAL BATH DEPOSITION AT DIFFERENT TEMPERATURES

P.E. RODRÍGUEZ-HERNÁNDEZ[a], F. DE MOURE-FLORES[a,*], A. GUILLÉN-CERVANTES[b], E. CAMPOS-GONZÁLEZ[a], J. SANTOS-CRUZ[a], S.A. MAYÉN-HERNÁNDEZ[a], J.S. ARIAS-CERÓN[c], M. DE LA L. OLVERA[c], O. ZELAYA-ÁNGEL[b], G. CONTRERAS-PUENTE[d].

[a]*Facultad de Química, Materiales, Universidad Autónoma de Querétaro, Querétaro, 76010, México.*

[b]*Departamento de Física, CINVESTAV-IPN, Apdo. Postal 14-740, México D.F. 07360, México.*

[c]*Departamento de Ingeniería Eléctrica, Sección de Estado Sólido, CINVESTAV-IPN, Apdo. Postal 14-740, México D.F. 07360, México.*

[d]*Escuela Superior de Física y Matemáticas del IPN, México D.F. 07738, México.*

Indium sulphide thin films were deposited on SnO_2:F/soda-lime glass substrates at different temperatures by chemical bath deposition. $InCl_3$ and C_2H_5NS were employed as indium and sulfur sources, respectively. The In_2S_3 films were deposited at temperatures of: 60 °C, 70 °C and 80 °C. The as-grown films were annealed at 300 °C in nitrogen atmosphere. The physical properties were analyzed as a function of the bath temperature, before and after the thermal treatment. The X-ray diffraction and Raman characterizations indicate that In_2S_3 films with tetragonal phase were obtained. Atomic force microscopy showed that after the annealing features of grain coalescence on surface are present. The UV-Vis analysis indicated that after thermal treatment In_2S_3 films have high transmission in the visible range and a bandgap above 2.50 eV.

(Received July 10, 2016; Accepted August 30, 2016)

Keywords: In_2S_3 films; Chemical bath deposition; Room temperature photoluminescence; Optical properties; Solar cells applications

1. Introduction

The development of low-cost processing techniques for the fabrication of photovoltaic materials and electronic devices is critical for cost-competitive photovoltaic electricity production in comparison with conventional sources of energy. Thin-film solar cells based on CdTe, CIGS and CZTS employ a CdS binary compound as window thin film layer. The replacement of CdS with other sulfides such as In_2S_3 has given good results. The indium sulphide (In_2S_3), a III-VI semiconductor compound, appears as a promising candidate for this application due to its stability, bandgap in the range 2.0-2.9 eV depending on its composition, and transparency [1]. Besides, In_2S_3 films have been used as substitute for CdS in thin film solar cells to avoid toxic cadmium and obtain more environment friendly photovoltaic technology [2]. Using a In_2S_3 layer replaces the toxic cadmium, besides the optical properties of the buffer layer are improved because this material has a bandgap wider than the one of CdS. In_2S_3 films have been grown by co-evaporation of In and S [3], electrochemical deposition [4], spray pyrolysis [5] and chemical bath deposition (CBD) [6]. The CBD technique is very attractive due to its feasibility to produce at low cost large-area thin films [7]. In this work, we report the influence of the growth temperature on physical properties of In_2S_3 films grown by CBD.

* Corresponding author: fcomoure@hotmail.com

2. Experimental details

2.1 Growth of In_2S_3 films

In_2S_3 films were deposited on commercial SnO_2:F/soda lime-glass (10 Ω/□ and 0.5 μm) substrates by CBD at different temperatures: 60 °C, 70 °C and 80 °C for 1 h. The reaction solution was prepared mixing 20 ml of 0.025 M $InCl_3$, 0.075 M C_2H_5NS (thioacetamide) and acetic acid. Deionized water (DI water-18 MΩ) was used for the preparation of solutions. The $InCl_3$ and C_2H_5NS were employed as indium and sulfur sources, respectively. The acetic acid formed complexes in the reaction process and maintained a pH of 3. The temperature was controlled with a hot plate equipped with magnetic stirrer. After deposition, films were rinsed in distilled water in ultrasonic bath for 5 min. Then, as-grown In_2S_3 films were heated at 300 °C in nitrogen atmosphere for 1 h. In_2S_3 thin films were labeled according to the bath temperature, see Table 1.

The decomposition of thioacetamide in an aqueous medium is as follows [1,8]:

$$CH_3CSNH_2 \leftrightarrow CH_3C(SH)NH$$

The protonation from acetic acid forms: $CH_3C(SH)NH + H^+ \leftrightarrow CH_3C(H_2S^+)NH$, which dissociates to give H_2S:

$$CH_3C(H_2S^+)NH \rightarrow CH^3CNH^+ + H_2S$$

In aqueous medium, H_2S dissociates to produce:

$$H_2S + H_2O \rightarrow HS^- + H_3O^+$$
$$HS^- + H_2O \rightarrow S^{2-} + H_3O^+$$

Then, ion-by-ion deposition mechanism between indium and sulfur ions takes place:

$$2In^{3+} + 3S^{2-} \rightarrow In_2S_3$$

2.2 Characterization

X-ray diffraction (XRD) patterns were obtained with a Rigaku Smartlab diffractometer, using the Cu-Kα line (1.5406 Å). XRD patterns were collected at a grazing-incidence of 1.5º, with a step size of 0.02º and a step time of 1 s. Raman spectroscopy measurements were carried out in a Labram Dilor micro-Raman system, employing a HeNe laser (632.8 nm) as excitation source. The morphology studies were performed by Atomic Force Microscopy (AFM), using a ThermoMicroscope Autoprobe CP Research AP-2001 in contact mode. Atomic concentration measurements of films were determined by Energy Dispersive Spectrometry (EDS) with a Bruker 5010 X-Flash detector installed in a JEOL JSM-6300 scanning electron microscope. Film thicknesses were measured in a KLA Tencor P15 profilometer. A Perkin-Elmer Lambda 25 UV-Vis spectrophotometer was used to obtain optical transmittance. Photoluminescence (PL) spectra were obtained at room temperature using an Omnichrome-Series 56 He-Cd laser emitting at 325 nm. The radiative emission from the samples was focused to the entrance slit of a HRD-100 Jobin-Yvon double monochromator with a resolution better than 0.05 nm and detected with an Ag-Cs-O Hamamatsu photomultiplier.

3. Results and discussion

3.1 Structural characterization

Fig. 1 shows XRD patterns of In_2S_3 films grown at different temperatures (60 °C, 70 °C and 80 °C) by CBD, before and after the annealing. Fig. 1a) shows the XRD diffractograms of as-grown In_2S_3 films. The sample deposited at 60 °C has three diffraction peaks at 27.70°, 33.45° and 48.00°, which correspond to In_2S_3 cubic or tetragonal phase. The diffraction planes are (311)C/(109)T, (400)/C(0012)T and (440)C/(2212)T, respectively. The diffraction peaks were

indexed using the power diffraction files (PDF) 32-0456 and 25-0390. From XRD patterns in Fig. 1a), note that the intensity of diffraction peaks decreases as the temperature of the bath increases, indicating a reduction in the crystalline quality of In_2S_3 films; in fact the film grown at 80 °C is practically amorphous. Fig. 1b) shows diffractograms of In_2S_3 films after the heat treatment. The In_2S_3-60°C film, after the annealing, has three additional diffraction peaks at 36.38°, 38.08° and 51.78°, which correspond to In_2S_3 cubic or tetragonal phase and diffraction planes are: (311)C/(303)T, (421)C/(1013)T and (610)C/(415)T, respectively. After the annealing, the diffractogram of the In_2S_3-80°C film has three additional diffraction peaks at 27.70°, 33.45° and 43.82°, the peak at 43.82° may correspond to In_2S_3 cubic or tetragonal, and the diffraction plane is (511)C/(1015)T, other peaks were discussed above. The annealing produces the presence of additional diffraction peaks, this may be due to a crystallization of amorphous material during the annealing. The crystallite size was calculated using the Scherrer formula: $D = 0.9\lambda/B\cos\theta_B$, where D is the crystallite size, λ is the XRD wavelength (1.5406 Å), B is the full width at half maximum (FWHM) of diffraction peak and θ_B is the Bragg angle. The crystallite size of each film, before and after the thermal treatment, is shown in Table 1. The crystallite size of In_2S_3-60°C film has a value of 22.05 nm, for a growth temperature of 70 °C the crystallite size was 25.59 nm and the In_2S_3-80°C as-grown sample has an average crystallite size of 17.65 nm. Note that after the annealing in nitrogen, the crystallite size decreases for all samples (see Table 1). The film thicknesses, before and after of the thermal treatment, are displayed in Table 1. The thickness of as-grown films are in the range of 149-188 nm. After the annealing in nitrogen the thickness of In_2S_3 films have a reduction of approximately 8%. The thickness for the In_2S_3 films in this work is in the range used in the processing of solar cells [9].

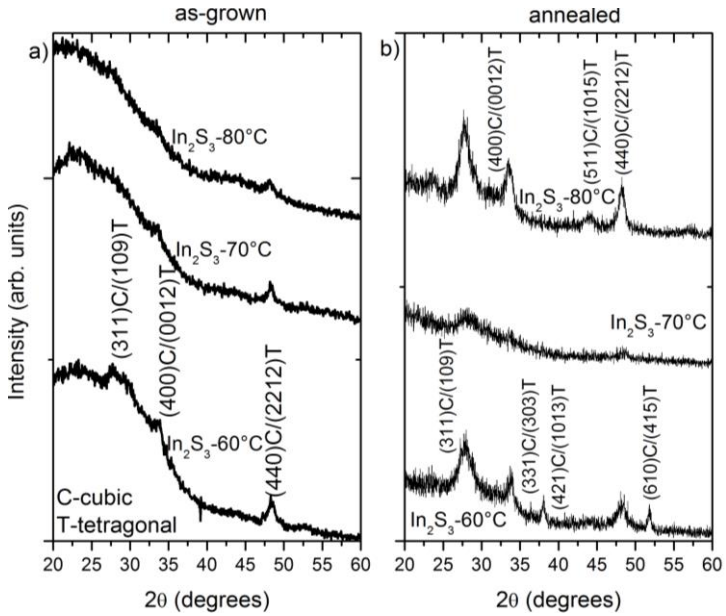

Fig.1. XRD patterns of In_2S_3 thin films grown by CBD for 60 min and different temperatures; 60 °C, 70 °C and 80 °C.

Table 1. Growth parameters, crystallite size and thickness of In_2S_3 films.

		As-grown		Annealed	
Sample	Bath temperature (°C)	Crystallite size (nm)	Thickness (nm)	Crystallite size (nm)	Thickness (nm)
In_2S_3-60°C	60	22.05	149	13.86	138
In_2S_3-70°C	70	25.59	188	14.76	172
In_2S_3-80°C	80	17.65	182	18.23	169

Raman spectra of In_2S_3 thin films grown at different temperatures are shown in Fig. 2. In_2S_3 films have three Raman peaks at 115 cm^{-1}, 135 cm^{-1} and 180 cm^{-1}, the signals correspond to tetragonal phase of the In_2S_3 (β-In_2S_3) [10,11]. The In_2S_3-60°C has an additional shoulder of lower intensity at 379 cm^{-1}, corresponding to In_2O_3 [12]. The In_2S_3-80°C sample has an additional peak at 305 cm^{-1}, assigned to β-In_2S_3 phase [10]. After heating the samples have a better definition in the β-In_2S_3 peaks located at 115 cm^{-1}, 135 cm^{-1} and 180 cm^{-1} can be observed in all the samples, note also the In_2O_3 peak detected in the In_2S_3-60°C film has disappeared. It is important to mention that the Raman analysis did not detect any peaks due to cubic phase (α-In_2S_3). Therefore, this analysis shows that In_2S_3 films grown by CBD have a tetragonal phase (β-In_2S_3).

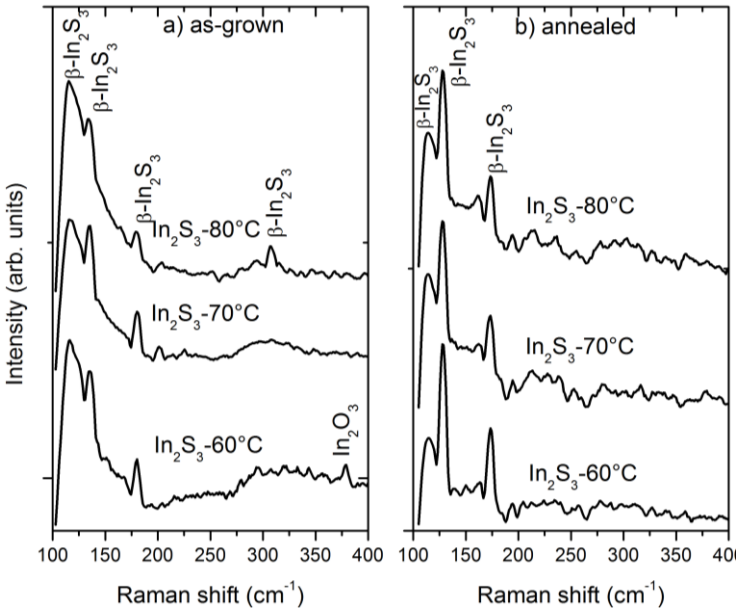

Fig. 2. Raman spectra of In_2S_3 films grown at different temperatures; 60 °C, 70 °C and 80 °C.

3.2 Atomic force microscopy characterization

Fig. 3 shows AFM (4 μm^2) images of In_2S_3-60°C and In_2S_3-80°C films, before and after the annealing in nitrogen at 300 °C. Note that the annealing produces a coalescence of grains in both samples. Figs. 3a-b) show the topography of the In_2S_3-60°C sample before and after the annealing, respectively. The root mean square (rms) roughness of In_2S_3-60°C as-grown and In_2S_3-60°C annealed films was 4.04 nm and 3.26 nm, respectively. The rms roughness of the In_2S_3-80°C film, before and after the heat treatment (Figs. 3c-d), was 4.03 nm and 3.75 nm, respectively. Thus, in general the annealing in nitrogen produces a coalescence of grains and reduces the rms roughness of In_2S_3 films grown by CBD. The conversion efficiency of solar cells is a parameter that strongly depends on the low roughness of buffer films used to manufacture such devices, remarking that the smallest rms roughness is obtained by this technology [13].

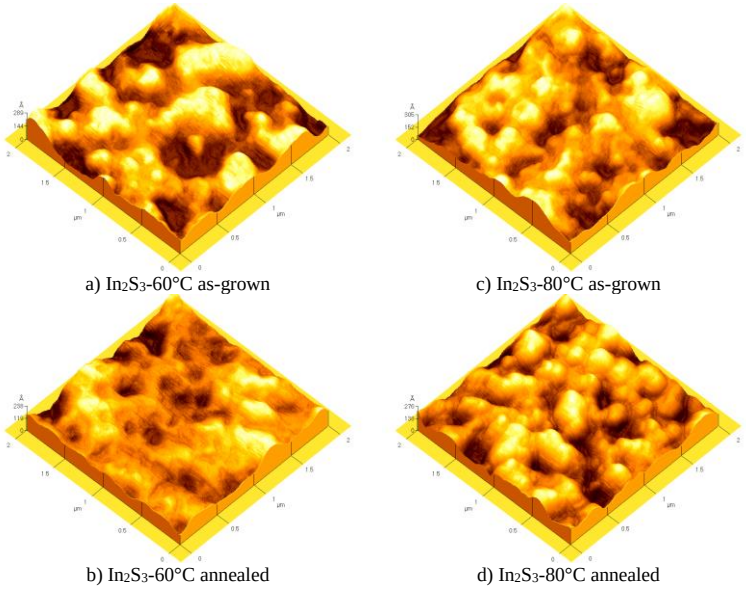

Fig. 3. AFM images of In_2S_3 films grown at 60°C and 80 °C before and after of the annealing.

3.3 Compositional characterization

In order to determine the composition of In_2S_3 thin films grown by CBD, EDS measurements were performed. In Table 2 the In and S atomic concentrations as well as the S:In ratio are listed. The In_2S_3-60°C as-grown film has a S:In ratio of 1.51, which is approximately the stoichiometry of the In_2S_3 compound. After heat treatment the S:In ratio of the In_2S_3-60°C has a value of 1.31, which is due to a lower vapor pressure of S respect to In. This analysis indicates that for a growth temperature of 60 °C In_2S_3 films with good stoichiometry were obtained, in agreement with those results of XRD and Raman.

Table 2. Bandgap (E_g) and In and S atomic concentrations of In_2S_3 films before and after annealing.

	As-grown				Annealed			
Sample	E_g (eV)	In (%)	S (%)	S:In	E_g (eV)	In (%)	S (%)	S:In
In_2S_3-60°C	2.27	39.81	60.19	1.51	2.56	43.35	56.65	1.31
In_2S_3-70°C	2.71	41.96	58.04	1.38	2.89	43.60	56.40	1.29
In_2S_3-80°C	2.32	32.17	67.83	2.11	2.52	38.14	61.86	1.62

3.4 Optical characterization

The optical transmittance spectra of In_2S_3 films grown by CBD at different temperatures, before and after heat treatment, are shown in Fig. 4. The transmittance of In_2S_3 as-grown films are shown in Fig. 4a), the In_2S_3-70°C as-grown film has the higher transmittance; between 60% and 75 % in the visible region (400-700 nm), which is suitable for solar cells applications. The transmittance of In_2S_3 films after heat treatment increases in 10%, which is due to the reduction of film thicknesses during the heat treatment. The absorption coefficient (α) was calculated by the relation: $T=(1-R)^2\exp(-\alpha d)$, where T is the transmittance, R the reflectance and d the film thickness. The absorption coefficient was used to determine the bandgap (E_g) for each film using the direct bandgap semiconductor relation $\alpha h\upsilon=(h\upsilon-E_g)^{1/2}$, where $h\upsilon$ is the photon energy. Fig 5 shows the graphic of $(\alpha h\upsilon)^2$ vs $h\upsilon$, E_g was calculated by fitting the lineal part of the curve. Bandgap values, before and after of the heat treatment, are displayed in Table 2. The In_2S_3-60°C as-grown sample

has a bandgap value of 2.27 eV. The In_2S_3-70°C and In_2S_3-80°C as-grown samples have an E_g of 2.71 eV and 2.32 eV, respectively. The E_g value of In_2S_3 annealed films increases about 8%, this increase in the E_g may be due to change in the crystallite size [14].

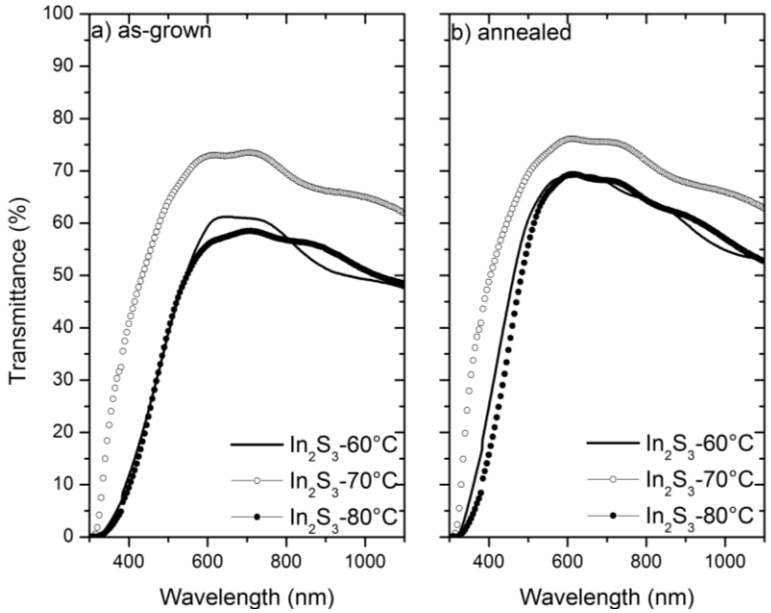

Fig.4 Transmittance spectra of In_2S_3 films deposited by CBD at different temperatures; 60 °C, 70 °C and 80 °C.

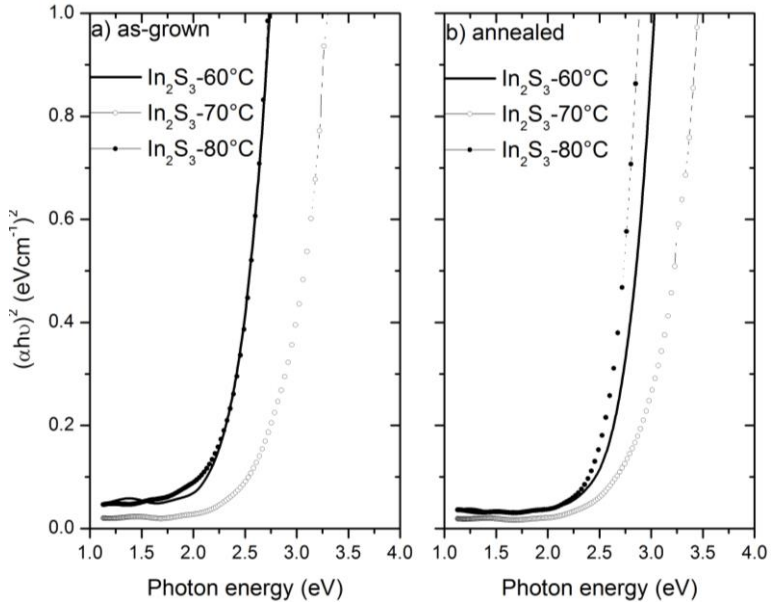

Fig. 5. Bandgap calculations for In_2S_3 films grown by CBD at different temperatures.

Fig. 6 shows the PL at room temperature of In_2S_3 films grown by CBD at different temperatures. In_2S_3 as-grown films have two emissions at 2.38 eV (high intensity) and 2.90 eV (low intensity), see Fig. 6. The green luminescence at 2.38 eV may be an emission from the indium interstitial sites, whereas the signal at 2.90 eV can be attributed to the presence of several deep trap states or defects in the In_2S_3 structure [12]. The PL of In_2S_3 films with annealing are shown in Fig. 6b). Observe that the signal at 2.90 eV attributed to defects disappears. After the annealing the PL spectra present two peaks at 1.74 eV (red emission) and the green emission

centered in 2.35 eV. The red emission is attributed to Donor-Acceptor Pair (DAP) recombination [15].

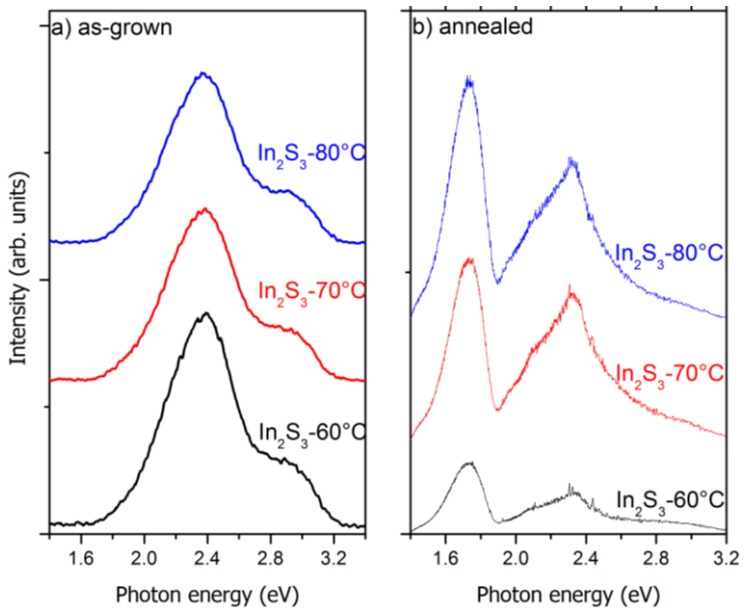

Fig. 6. Photoluminescence spectra at room temperature of In_2S_3 thin films grown at different temperatures: 60 °C, 70 °C and 80 °C.

4. Conclusions

In_2S_3 thin films by chemical bath deposition at different temperatures were obtained. The structural and optical properties were analyzed as a function of growth temperature. The structural characterization (XRD and Raman) showed that In_2S_3 films have tetragonal phase (β-In_2S_3). The XRD showed that for a growth temperature of 60 °C the best polycrystalline quality was obtained, when the growth temperature increases the crystalline quality degrades. In_2S_3 films has high transmittance; between 60% and 75% which is suitable for photovoltaic applications. The structural and morphology analysis showed that the annealing in nitrogen produces a crystalline coalescence of grains which reduces the rms roughness of In_2S_3 thin films. The optical bandgap increases after the annealing, which is due to change of crystallite size produced during the thermal treatment. The PL signal attributed to defects disappears after the thermal treatment, which indicates an improvement in the crystalline quality of In_2S_3 thin films grown by chemical bath deposition.

Acknowledgments

We acknowledge the technical support of Marcela Guerrero, A. Garcia-Sotelo, Rogelio Fragoso, Zacarías Rivera (from the Physics Department, CINVESTAV-IPN), Benito Ortega and the partial support by SEP-PRODEP DSA/103.5/15/6976.

The authors acknowledge financial support for this work from FONDO SECTORIAL CONACYT-SENER-SUSTENTABILIDAD ENERGÉTICA through CeMIE-sol, within of the strategic project number 37; “Development of new photovoltaic devices and semi-superconductor materials”.

References

[1] Indra Puspitasari, T.P. Gujar, Kwang-Deog Jung, Oh-Shim Joo, J. Mater. Proc. Tech. **201**, 775 (2008).
[2] J.F. Trigo, B. Asenjo, J. Herrero, M.T. Gutiérrez, Sol. Energy Mater. Sol. Cells **82**, 1145 (2008).
[3] C. Laurencic, L. Arzel, F.C. Devy, N. Barreau, Thin Solid Films **519**, 7553 (2011).
[4] A.M. Haleem, M. Ichimura, Thin Solid Films **516**, 7783 (2008).
[5] K. Otto, A. Katerski, A. Mere, O. Volobujeva, M. Krunks, Thin Solid Films **519**, 3055 (2011).
[6] B. Asenjo, C. Guillén, A.M. Chaparro, E. Saucedo, V. Bermudez, D. Lincot, J. Herrero, M.T. Gutiérrez, J. Phys. Chem. Solids 71, 1629 (2010).
[7] F. de Moure-Flores, K.E. Nieto-Zepeda, A. Guillén-Cervantes, S. Gallardo, J.G. Quiñones-Galván, A. Hernández-Hernández, M. de la L. Olvera, M. Zapata-Torres, Y. Kundriavtsev, M. Meléndez-Lira, J. Phys. Chem. Solids **74**, 611(2013).
[8] F. de Moure-Flores, A. Guillén-Cervantes, E. Campos-González, J. Santoyo-Salazar, J.S. Arias-Cerón, J. Santos-Cruz, S.A. Mayén-Hernández, M. de la L. Olvera, J.G. Mendoza-Álvarez, O. Zelaya-Angel, G. Contreras-Puente, Mater. Sci. Semicond. Process. **39**, 755 (2015).
[9] Ferhat Aslan, Getachew Adam, Philipp Stadler, Abdullah Goktas, Ibrahim Halil Mutlu, Niyazi Serdar Sariciftci, Solar Energy **108**, 230 (2014).
[10] K. Kambas, J. Spyridelis, M. Balkanski, Phys. Status Solidi b **105**, 291 (1981).
[11] E. Kärber, K. Otto, A. Katerski, A. Mere, M. Krunks, Mater. Sci. Semicond. Process. **25**, 137 (2014).
[12] Anuja Datta, Subhendu K. Panda, Dibyendu Ganguli, Pratima Mishra, Subhadra Chaudhuri, Cryst. Growth Des. **7**, 163 (2007).
[13] M. Tsuji, T. Aramoto, H. Ohyama, T. Hibino, K. Omura, Characterization of CdS Thin-Film in High Efficient CdS/CdTe Solar Cells, Jpn. J. Appl. Phys. **39**, 3902 (2000).
[14] N.S. Das, P.K.Ghosh, M.K.Mitra, K.K.Chattopadhyay, Physica E **42**, 2097 (2010).
[15] R. Jayakrishnan, Teny Theresa John, C. Sudha Kartha, K. P. Vijayakumar, Deepti Jain, L. S. Sharath Chandra, and V. Ganesan, J. App. Phys. **103**, 053106 (2008).